Exploring the Sun and its effects on the Earth's atmosphere and physical environment...

HIGH ALTITUDE OBSERVATORY

Subsurface Evolution of Emerging Magnetic Fields

Yuhong Fan (HAO/NCAR)

Outline

- Statement of the problem
- Overview of results from the thin flux tube model and from MHD simulations in local Cartesian geometries
- New preliminary results from 3D MHD simulations of emerging magnetic fields in a rotating spherical model solar convective envelope.
- New results on the post-emergence evolution of sunspot flux tubes based on similarity flux tube solutions: dynamic disconnection.

(from Cauzzi et al. 1996, Ap.J. 456, 850)

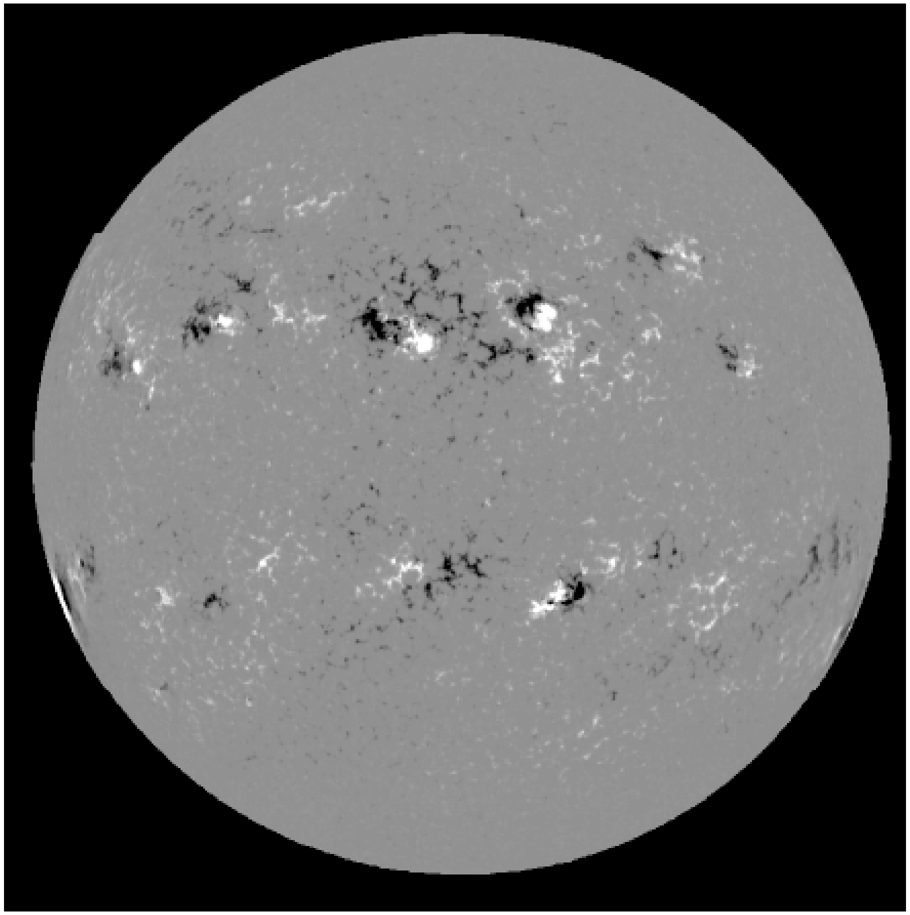

Full disk magnetogram from KPNO

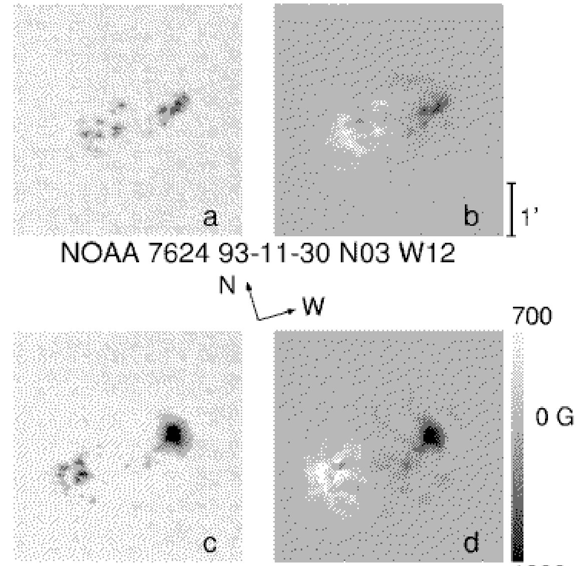

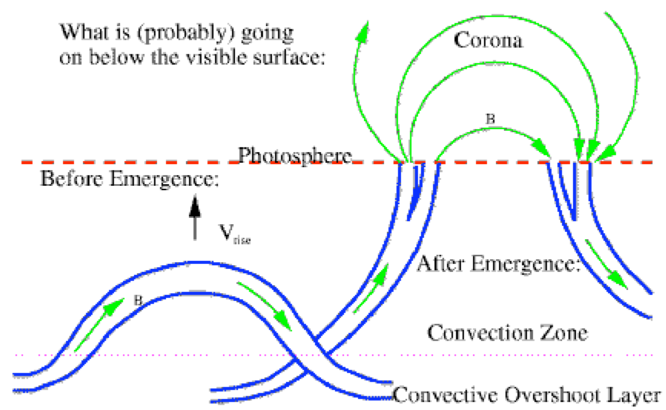

Figure by George Fisher

The Thin Flux Tube Model

- Thin flux tube approximation:

  $a << H_p$, all physical quantities are averages over the tube cross-section, solve for the mean motion of each tube segment under the relevant forces:

$$\rho \frac{d\mathbf{v}}{dt} = 2\rho(\mathbf{v}\times\mathbf{\Omega}) + (\rho - \rho_e)\mathbf{g}_{\text{eff}} + \hat{\mathbf{l}}\frac{\partial}{\partial s}\left(\frac{B^2}{8\pi}\right) + \frac{B^2}{4\pi}\mathbf{k} - C_D \frac{\rho_e |(\mathbf{v}_{\text{rel}})_\perp| (\mathbf{v}_{\text{rel}})_\perp}{\pi(\Phi/B)^{1/2}}$$

- Results:
  - Field strength of the toroidal magnetic field at the base of SCZ is of order $10^5 G$
  - Tilt of the emerging loop: active region tilts, Joy's law
  - Asymmetric inclination of the two sides of the emerging loop
  - Asymmetric field strength between the two sides of the loop

MHD Simulations in Local Cartesian Geometries

- The dynamic effects of field-line twist:
  - Maintaining cohesion of rising flux tubes

Fan et al. (1998)

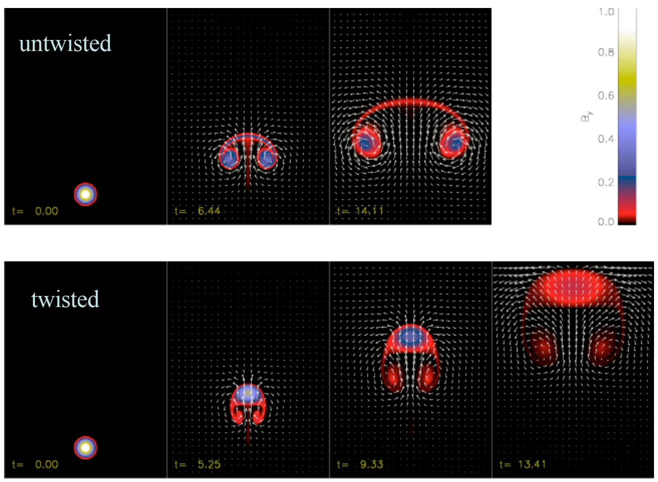

Abbett et al. (2001)

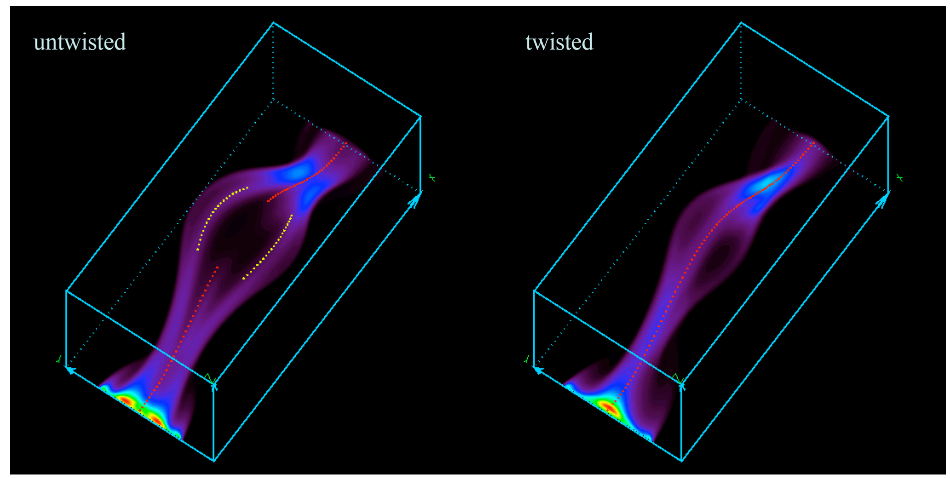

For 2D horizontal tubes: twist rate $q > (H_p a)^{-1/2}$, where $q \equiv B_\theta / rB_z$ (e.g. Moreno-Insertis & Emonet 1996, Fan et al. 1998; Longcope et al. 1999).

For 3D arched flux tubes: necessary twist may be less, depending on the initial conditions (e.g. Abbett et al. 2000; Fan 2001)…

NCAR

Fan (2001)

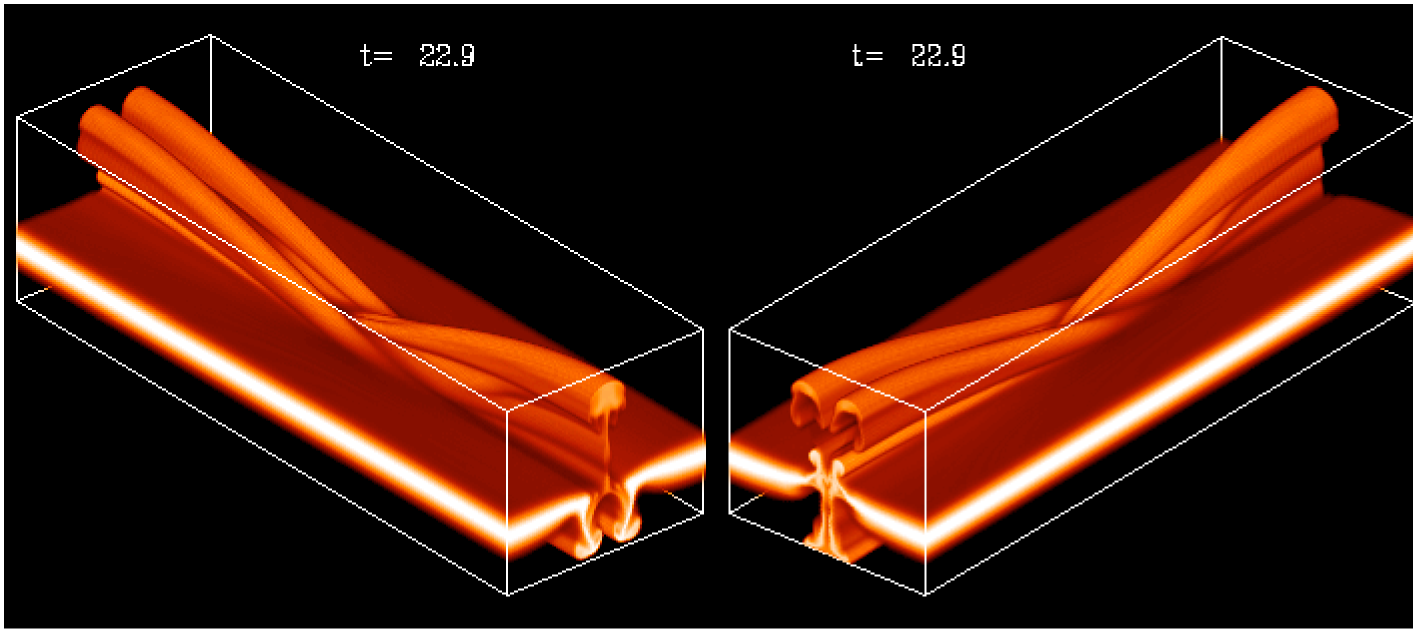

Apex cross-section

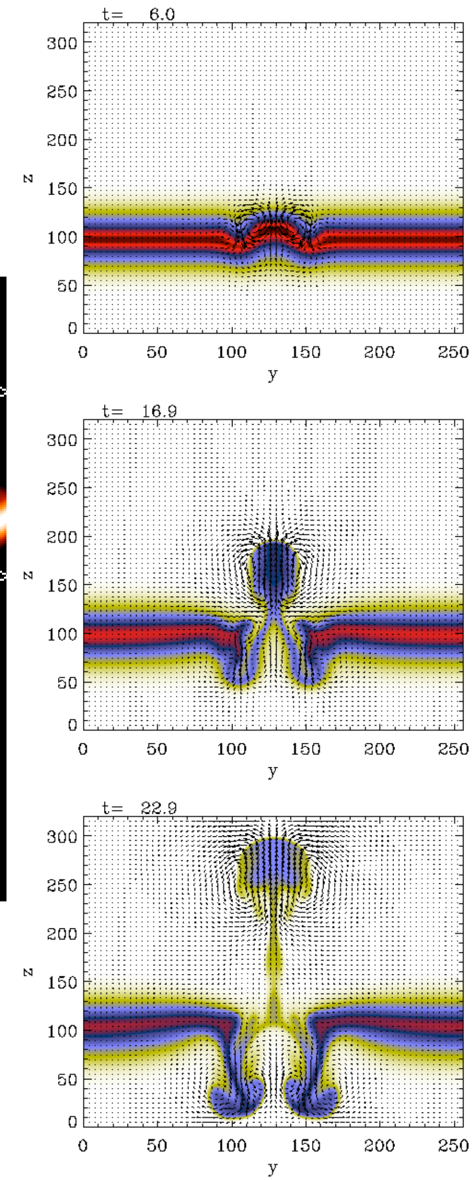

NCAR

- The dynamic effects of field-line twist (continued):

  – Becoming kink unstable when the twist is sufficiently high → formation of flare-productive delta-sunspot regions (e.g. Linton et al. 1998, 1999; Fan et al. 1999):

Fan et al. (1999)

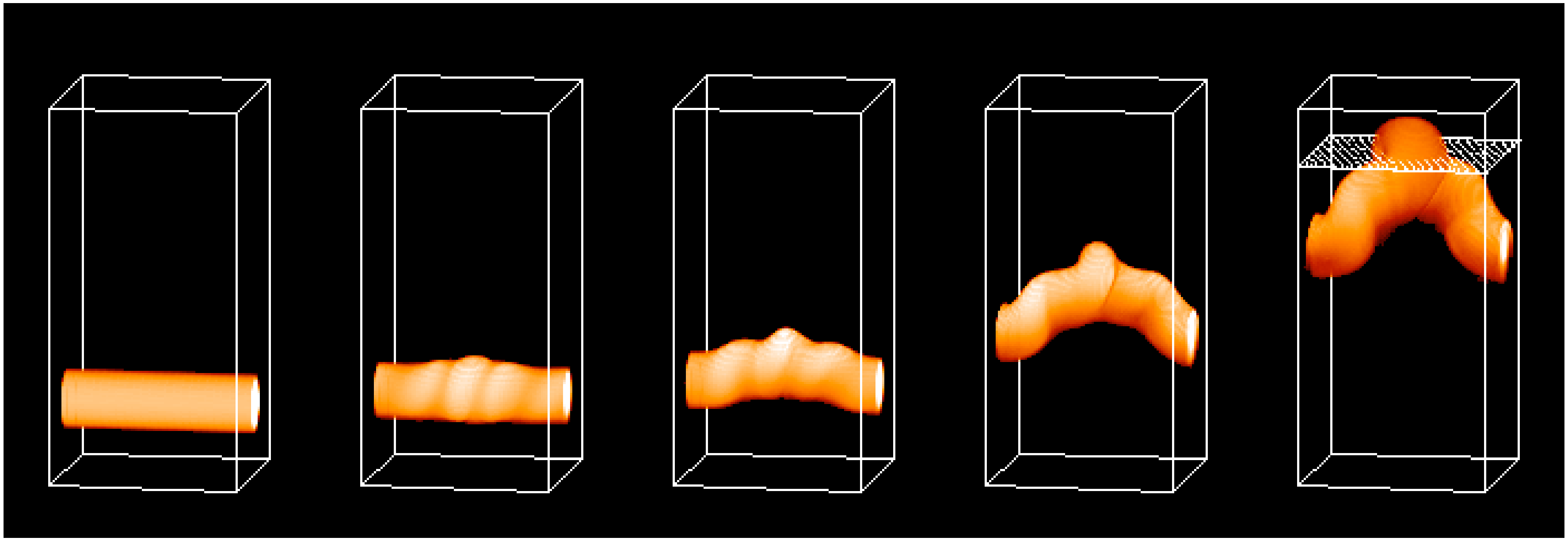

twist rate $q > a^{-1}$, where $q \equiv B_\theta / rB_z$ (Linton et al. 1996)

NCAR

Anelastic MHD Simulations in a Spherical Shell

- **In the bulk of the solar convection zone:**

$\delta \ll 1$, where $\delta = \nabla - \nabla_{\rm ad}$ with $\nabla = d\ln T/d\ln p$ and $\nabla_{\rm ad} = (d\ln T/d\ln p)_{\rm ad}$, thus $v/c_s \sim \delta^{1/2} \ll 1$.

$\beta \gg 1$, $v_a/c_s \ll 1$.

- **Anelastic Equations** :

$$\nabla \cdot (\rho_0 \mathbf{v}) = 0,$$

$$\rho_0 \left[\frac{\partial \mathbf{v}}{\partial t} + (\mathbf{v} \cdot \nabla)\mathbf{v} \right] = 2\rho_0 \mathbf{v} \times \mathbf{\Omega} - \nabla p_1 + \rho_1 \mathbf{g} + \frac{1}{4\pi}(\nabla \times \mathbf{B}) \times \mathbf{B},$$

$$\rho_0 T_0 \left[\frac{\partial s_1}{\partial t} + (\mathbf{v} \cdot \nabla)(s_0 + s_1) \right] = 0,$$

$$\nabla \cdot \mathbf{B} = 0,$$

$$\frac{\partial \mathbf{B}}{\partial t} = \nabla \times (\mathbf{v} \times \mathbf{B}),$$

$$\frac{\rho_1}{\rho_0} = \frac{p_1}{p_0} - \frac{T_1}{T_0},$$

$$\frac{s_1}{c_p} = \frac{T_1}{T_0} - \frac{\gamma - 1}{\gamma} \frac{p_1}{p_0},$$

where

$s_0(r)$, $p_0(r)$, $\rho_0(r)$, $T_0(r)$: the time-independent reference state of a hydrostatic, nearly adiabatically stratified spherical shell. JCD's solar model is used.

$\mathbf{v}$, $\mathbf{B}$, s_1, p_1, ρ_1, T_1: the dependent variables to be solved that describe the changes from the reference state.

Anelastic MHD Simulations in a Spherical Shell

We solve the above anelastic MHD equations in a spherical shell representing the solar convective envelope (which may include a sub-adiabatically stratified stable thin overshoot layer):

— staggered finite-difference

— two-step predictor-corrector time stepping

— An upwind, monotonicity-preserving interpolation scheme is used for evaluating the fluxes of the advection terms in the momentum equations

— A method of characteristics that is upwind in the Alfven waves is used for evaluating both the Lorentz force term and the V x B term in the induction equation (Stone & Norman 1992).

— The constrained transport scheme is used for advancing the induction equation to ensure that B remains divergence free.

— Solving the elliptic equation for p_1 at every sub-time step to ensure $\nabla \bullet (\rho_0 \mathbf{v}) = 0$

- FFT in the φ -direction → a 2D linear system for each azimuthal order m
- The 2D linear equatoin (in r, θ) for each azimuthal order m is solved with the generalized cyclic reduction scheme of Swartztrauber (NCAR's FISHPACK).

Anelastic MHD Simulations in a Spherical Shell

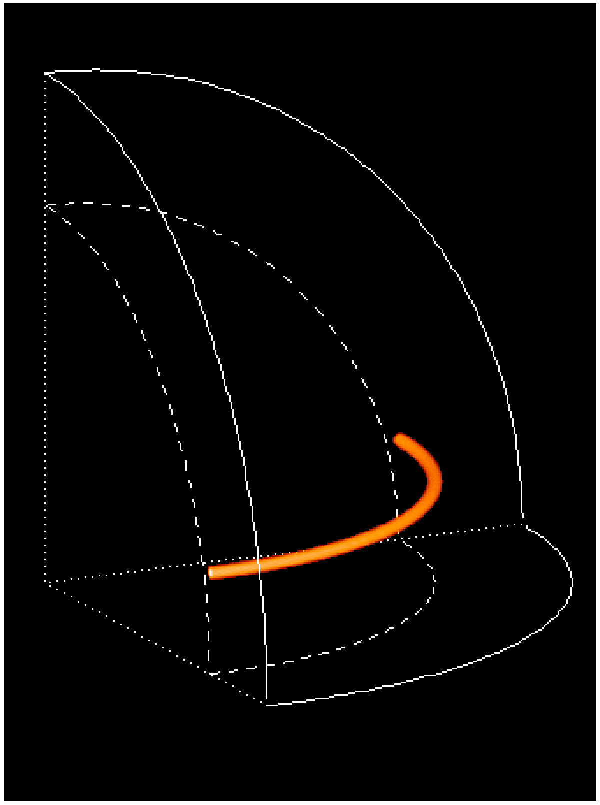

- Simulation domains:
  $r = [0.722R_\odot, 0.977R_\odot], \theta = [0, \pi/2], \phi = [0, \pi/2]$

- grid: $256 \times 512 \times 512$

- Reference state: JCD's solar model is used for $p_0(r)$, $\rho_0(r)$, $T_0(r)$, $g(r)$, and assuming $\delta = 0$, or $s_0(r) = 0$ (marginally stable for convection).

- Initial conditions: A twisted toroidal flux tube is placed at the base of the model convective envelope. The initial magnetic field is given by:

$$\mathbf{B} = \nabla \times \left(\frac{A(r,\theta)}{r \sin\theta} \hat{\phi} \right) + B_\phi(r,\theta)\hat{\phi}$$

with

$$A(r,\theta) = \frac{1}{2} q a^3 B_t \exp\left(-\frac{\varpi^2(r,\theta)}{a^2} \right)$$

$$B_\phi(r,\theta) = \frac{a B_t}{r \sin\theta} \exp\left(-\frac{\varpi^2(r,\theta)}{a^2} \right)$$

$$\varpi = (r^2 + r_0^2 - 2 r r_0 \cos(\theta - \theta_0))^{1/2}$$

where q is the rate of twist (angle per unit length), a is radius of the tube, r_0 is the r position of the initial tube, and θ_0 is the initial θ position of the tube.

An initial sinusoidal variation of entropy is imposed along the toroidal tube, such that the mid-point of the toroidal tube is buoyant, and the two ends are approximately in neutral buoyancy.

Case 1: $B_0 = 10^5 G, \quad q = 0.3a^{-1} \quad \lambda = 15^\circ.$

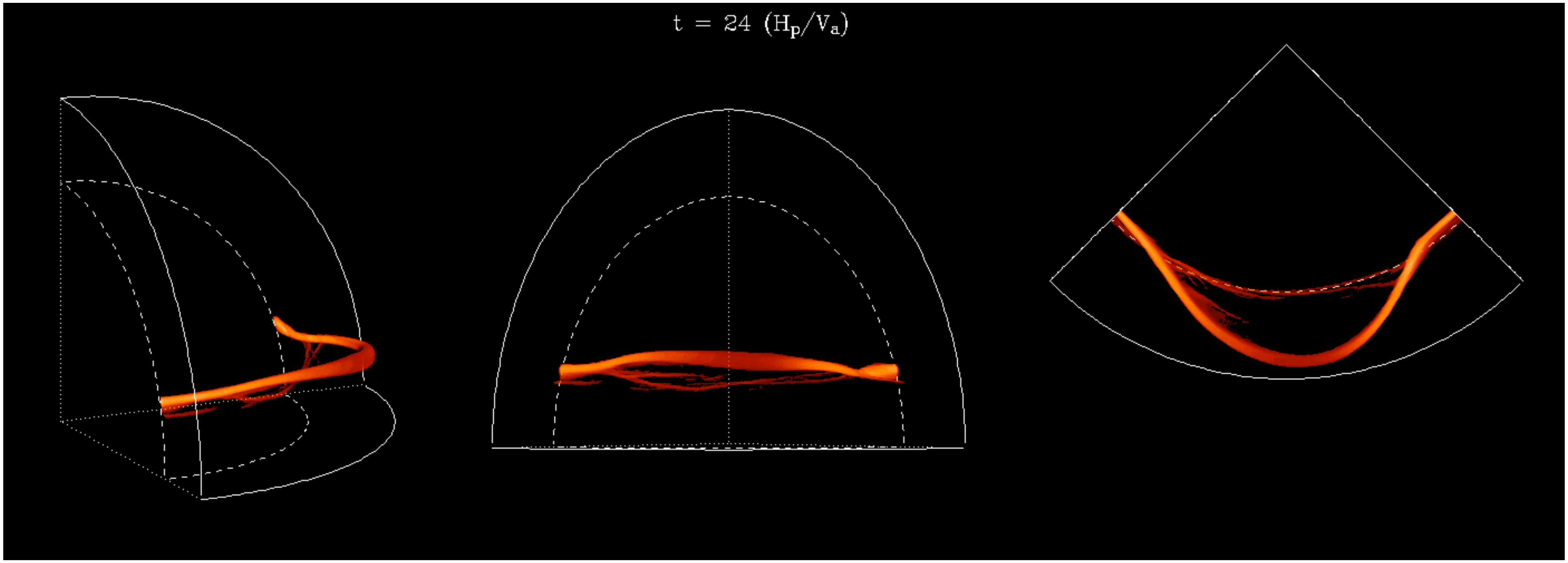

- Asymmetries:

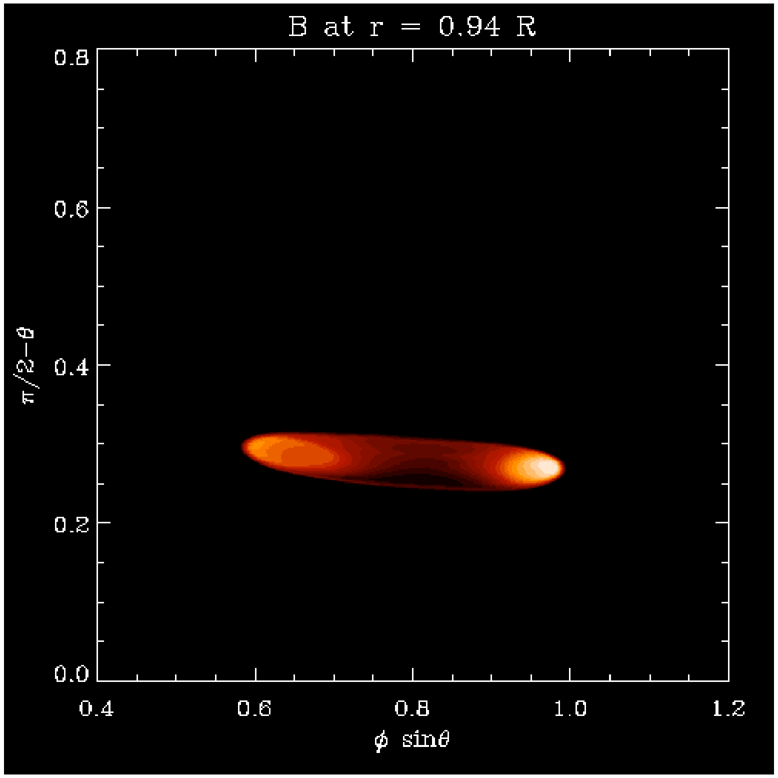

$tilt = 4.5^{o}$

$t = 24H_p / V_{A0}$

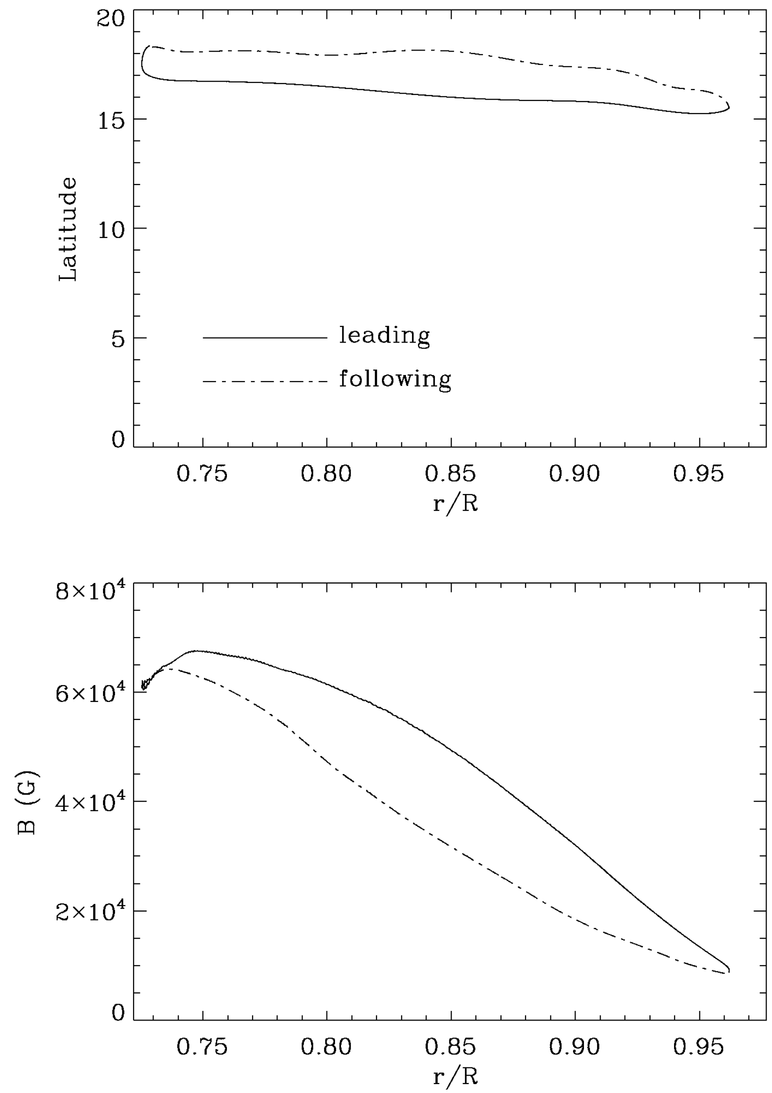

NCAR

- Origin of field strength asymmetry: asymmetric stretching due to the Coriolis force

$$\frac{d}{dt}\left(\frac{\mathbf{B}}{\rho}\right) = \left(\frac{\mathbf{B}}{\rho}\cdot\nabla\right)\mathbf{v}$$

$$\Longrightarrow \quad \frac{d\ln(\delta l)}{dt} \equiv \frac{d}{dt}\left(\frac{B}{\rho}\right) = \frac{\partial \mathbf{v}}{\partial l}\cdot\hat{\mathbf{l}}$$

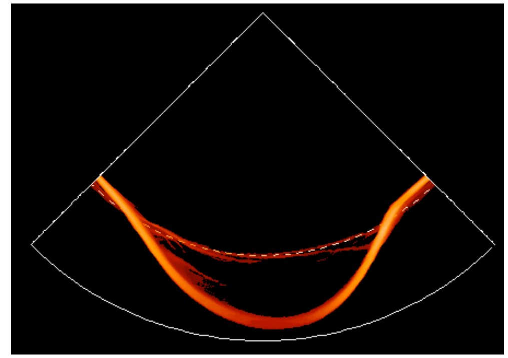

$t = 8H_p / V_A$

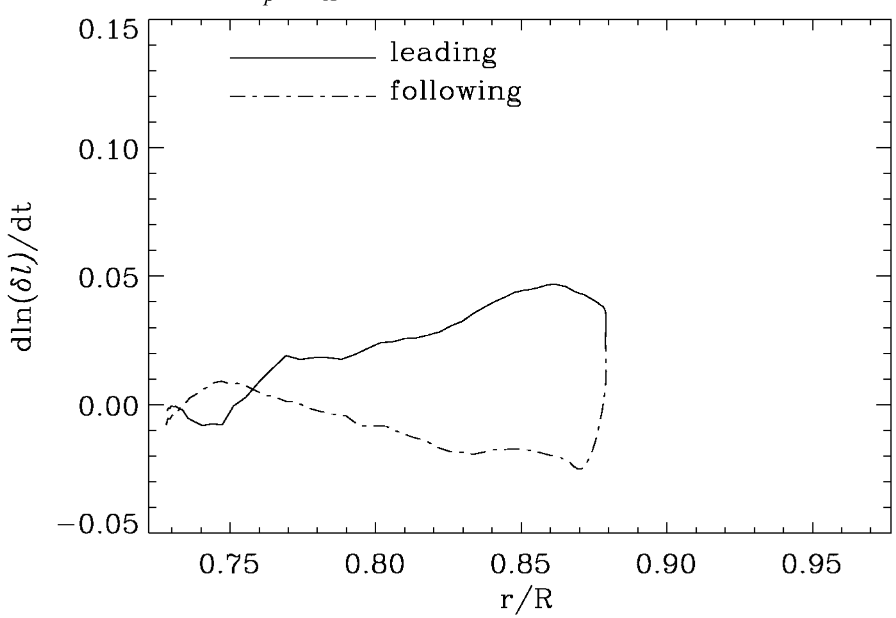

$t = 12H_p / V_A$

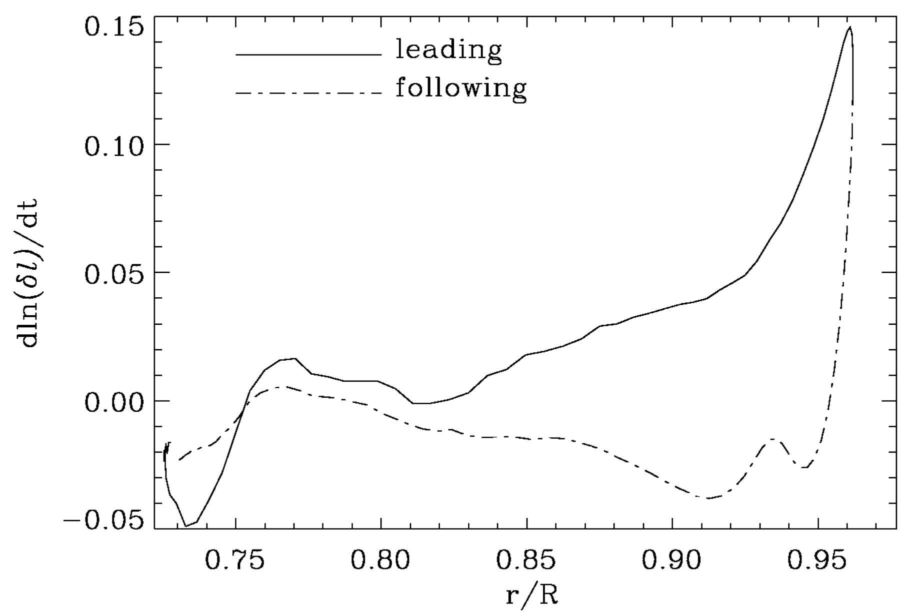

• Dependence on latitude:

$$B_0 = 10^5 G, \quad q = 0.3a^{-1} \quad \lambda = 30^{\circ}.$$

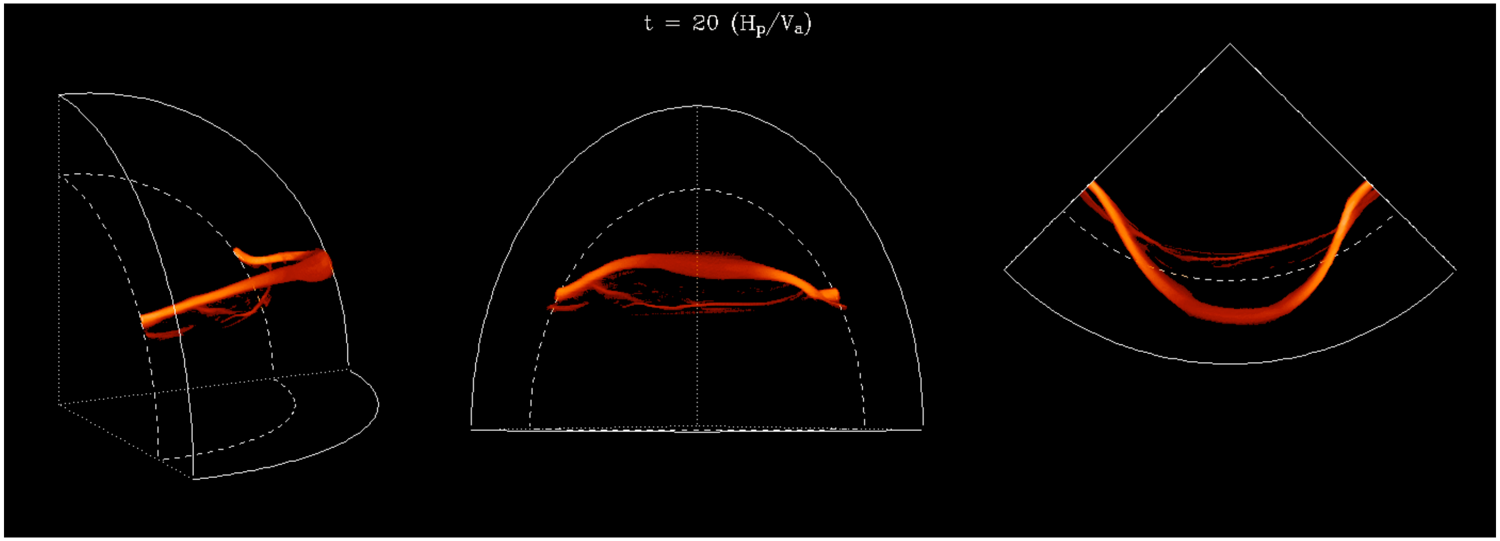

$$B_0 = 10^5 G, \quad q = 0.3a^{-1} \quad \lambda = 15^{\circ}.$$

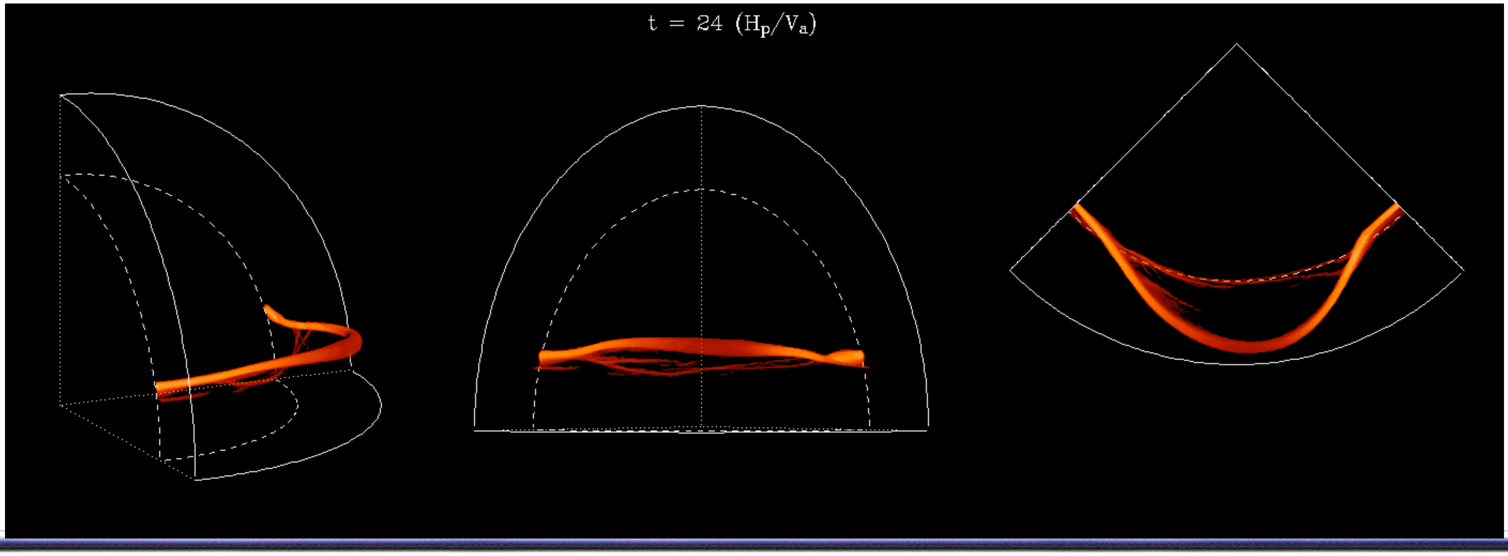

NCAR

• Dependence on latitude:

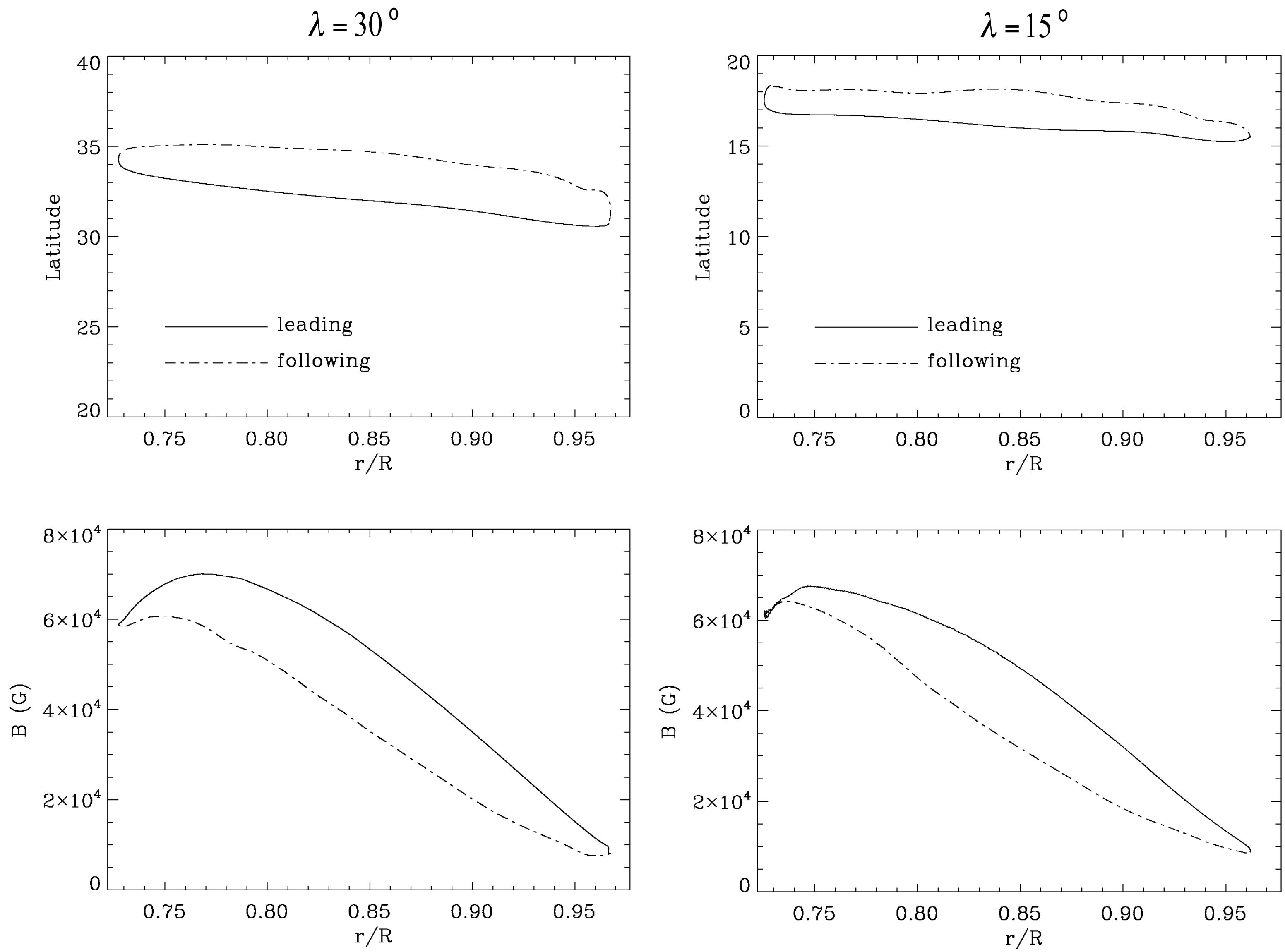

• Dependence on field strength:

$$B_0 = 5\times10^4 G, \quad q = 0.3a^{-1} \quad \lambda = 15^\circ.$$

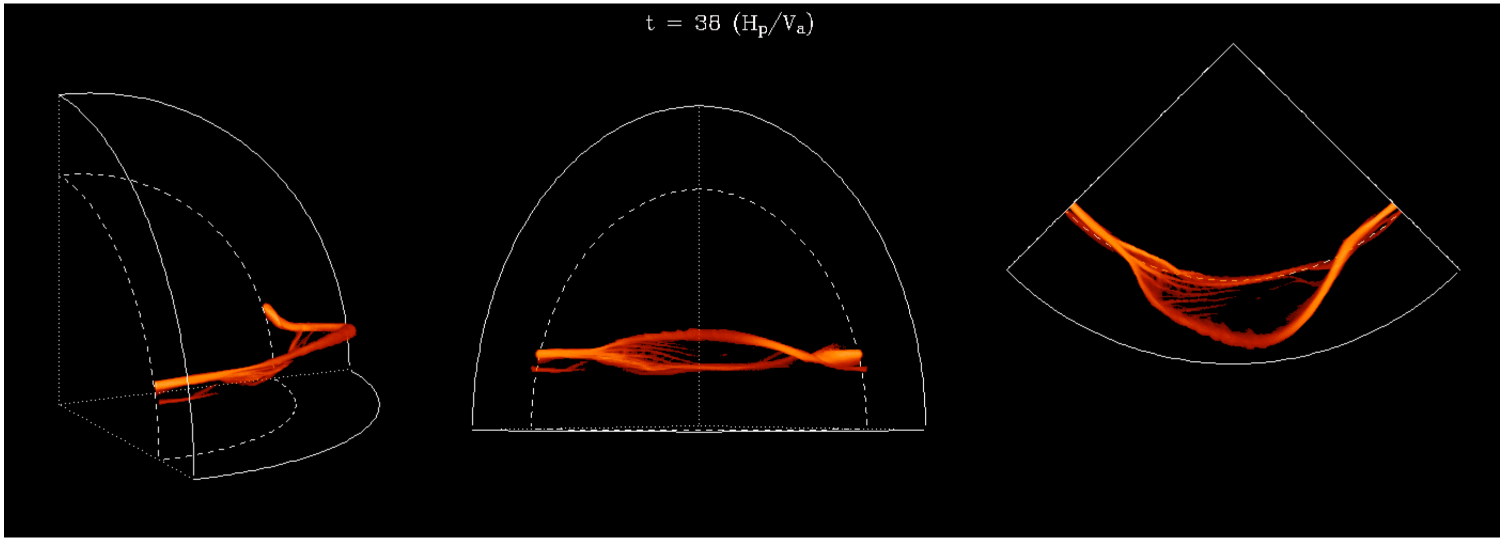

$$B_0 = 10^5 G, \quad q = 0.3a^{-1} \quad \lambda = 15^\circ.$$

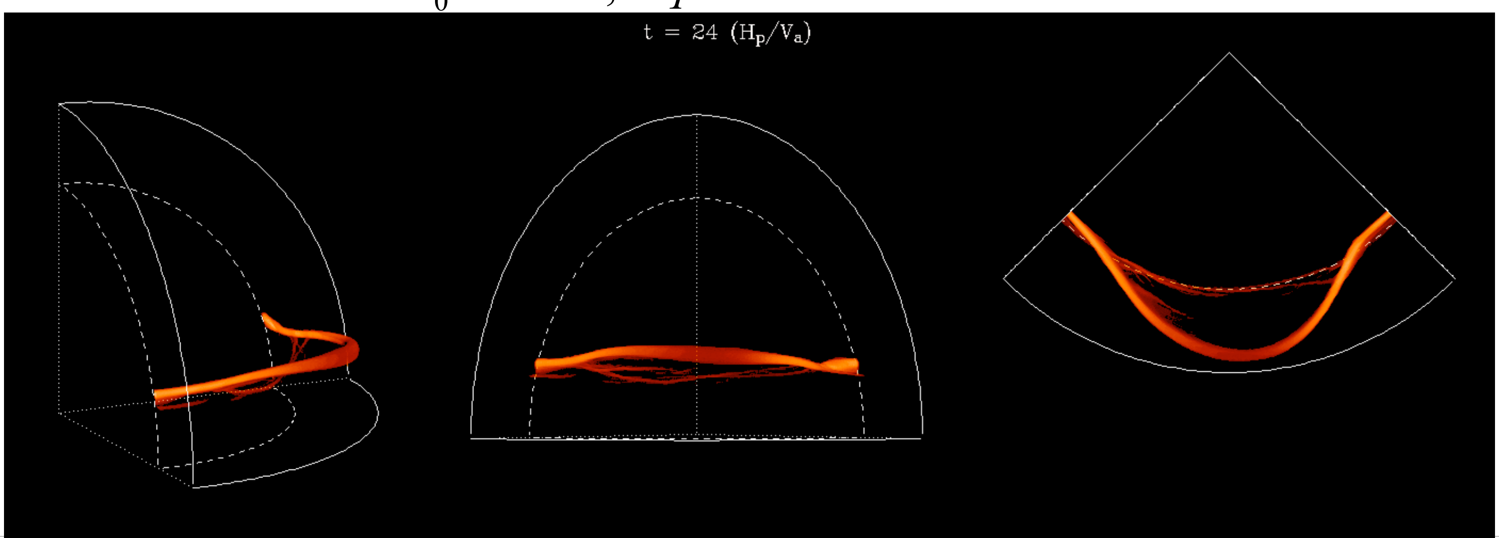

NCAR

• Dependence on field strength:

$B_0 = 10^5 G$

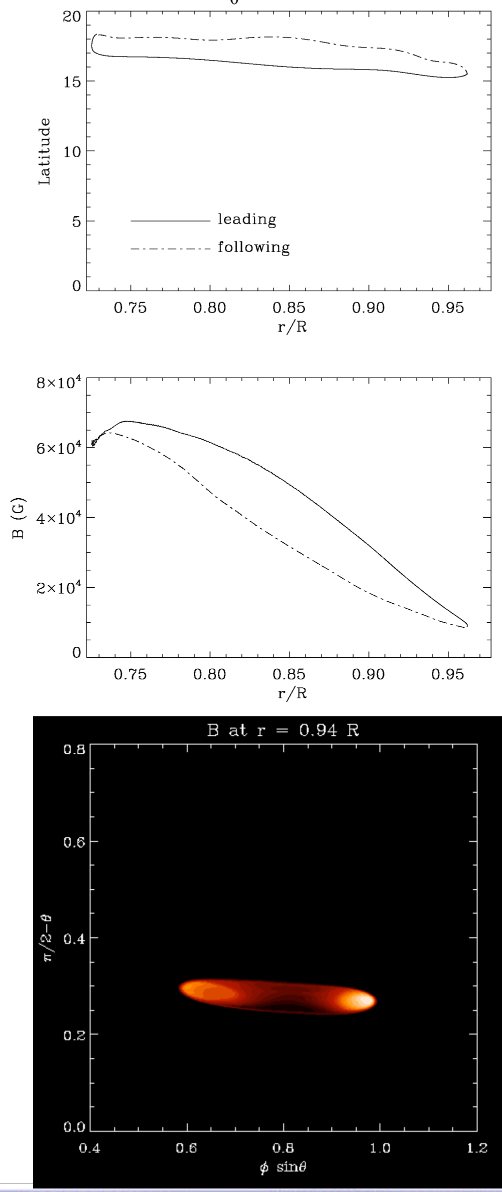

$B_0 = 5\times10^4 G$

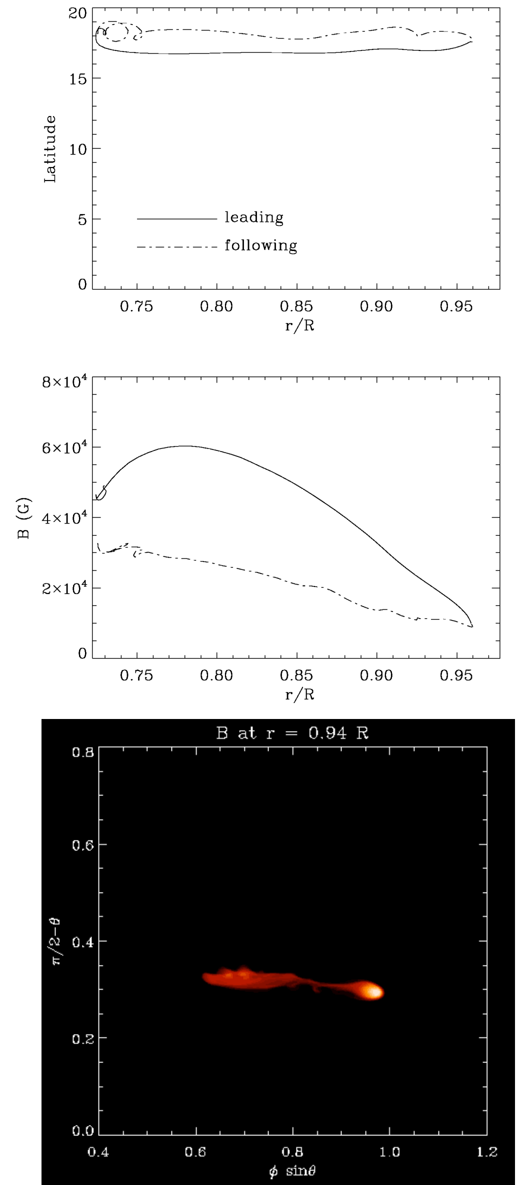

• Dependence on twist:

$$B_0 = 10^5 G, \quad q = 0 \quad \lambda = 15^\circ.$$

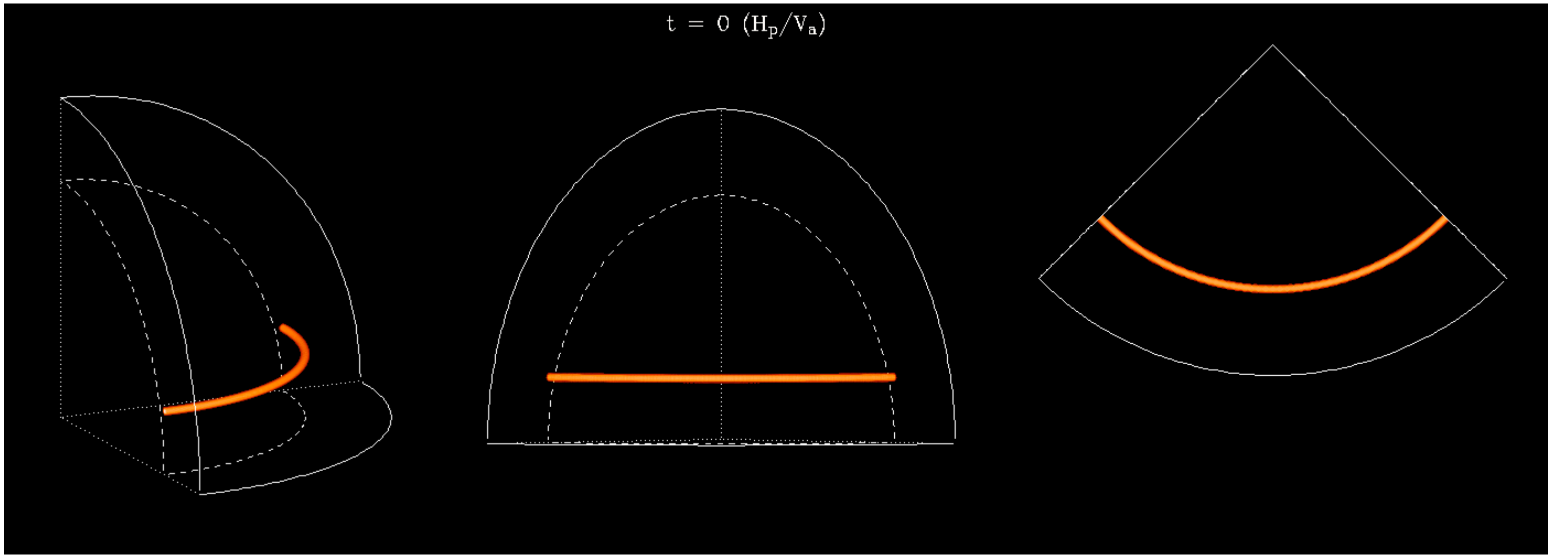

$$B_0 = 10^5 G, \quad q = 0.3a^{-1} \quad \lambda = 15^\circ.$$

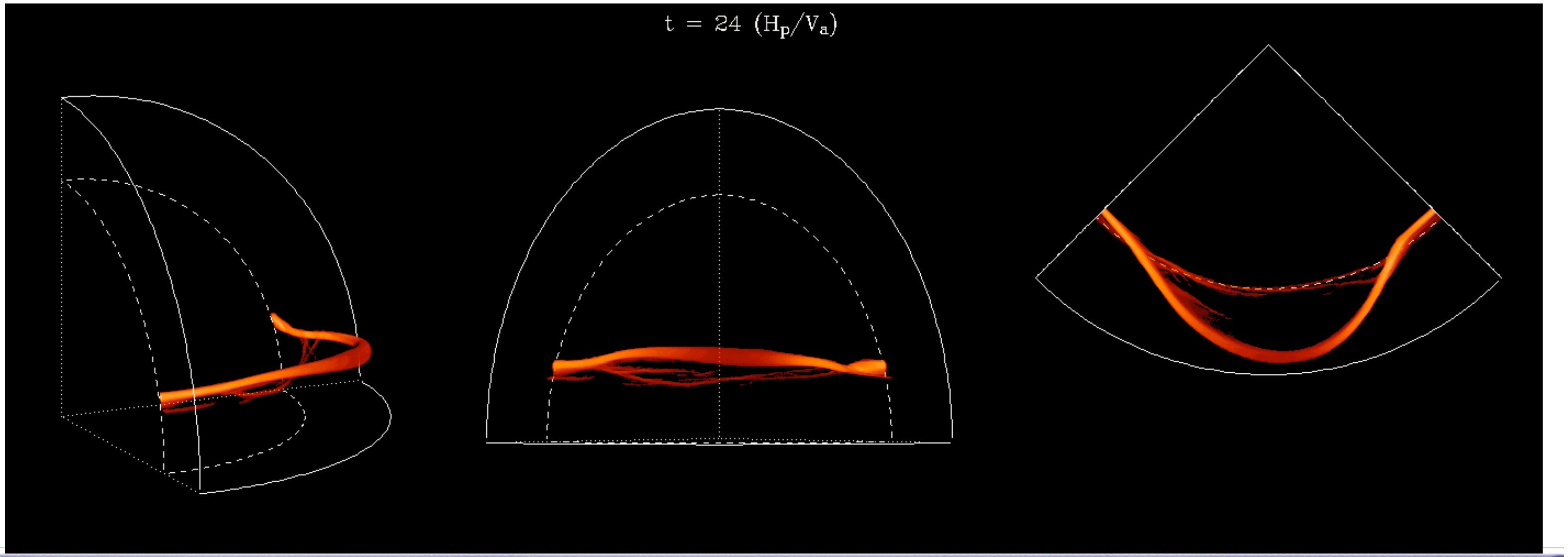

NCAR

• Dependence on twist:

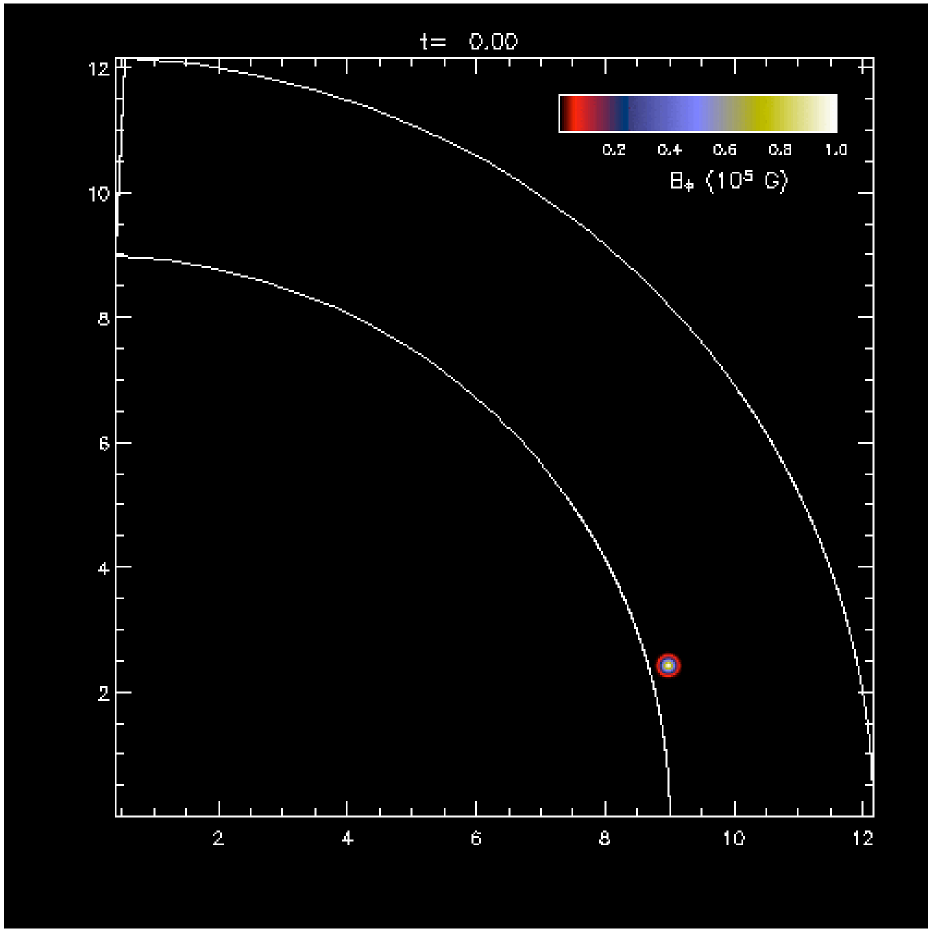

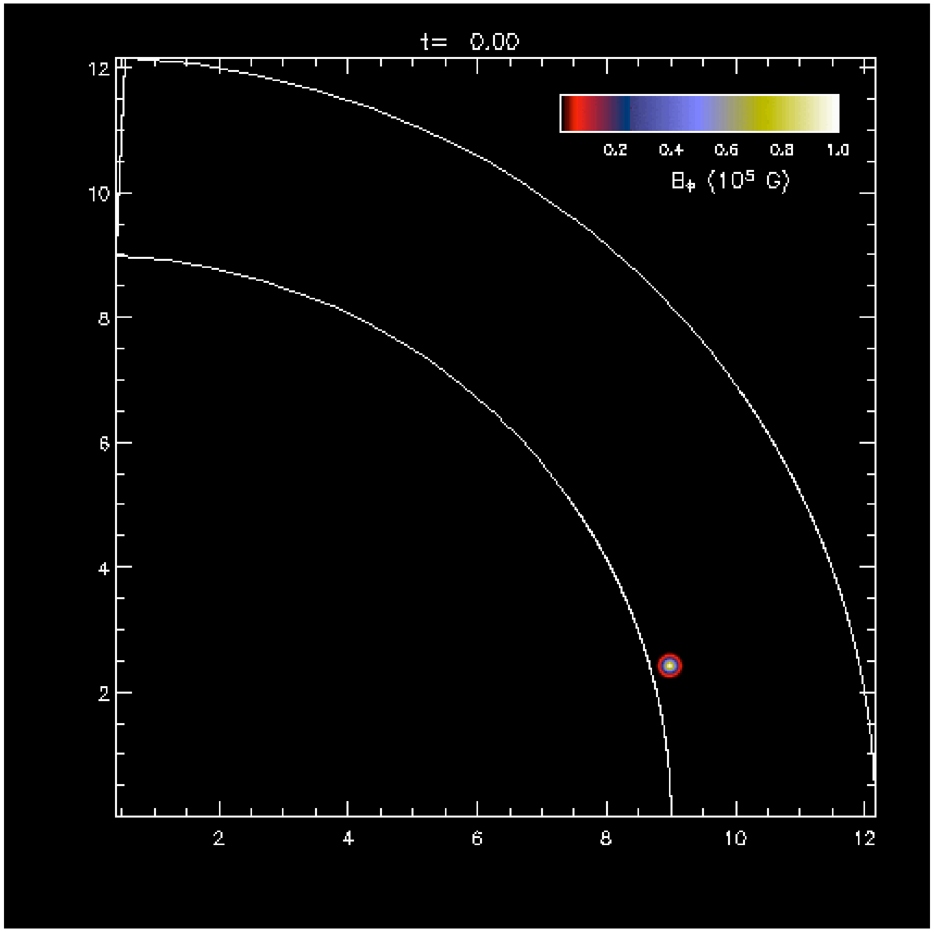

NCAR

The observed systematic twist in solar active regions

Pevtsov et al. (1995)

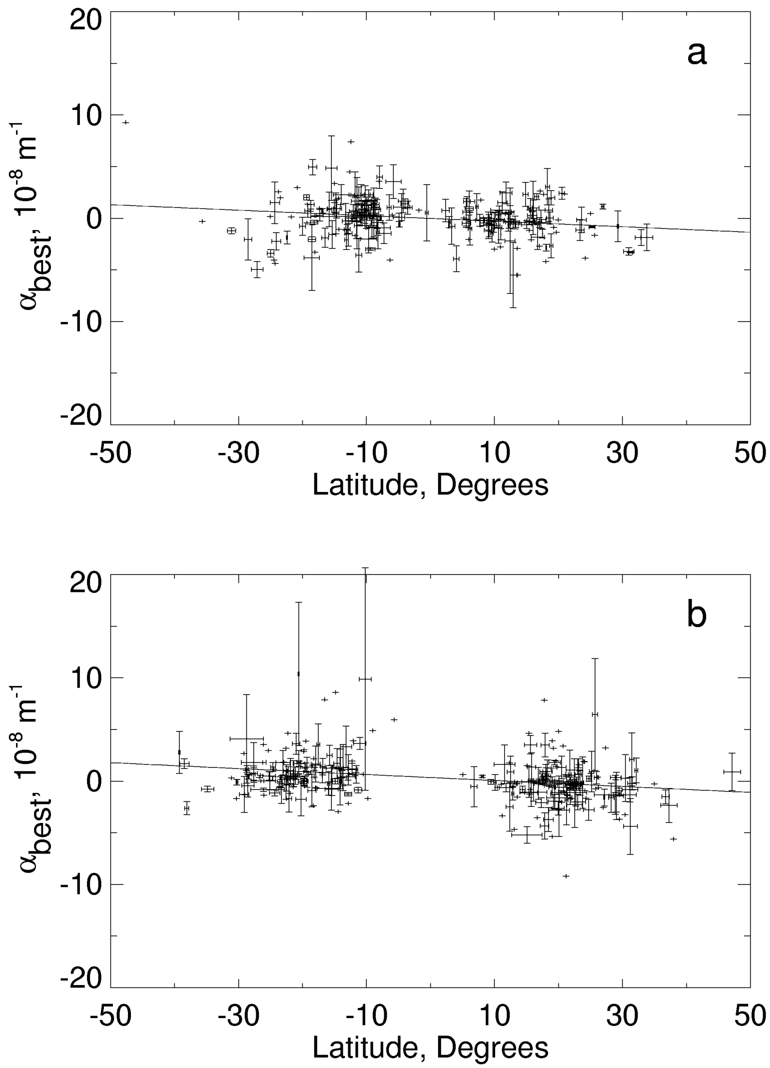

Assume thin flux tubes (Longcope and Klapper 1998, Longcope et al. 1998):

$$q = \alpha_{best} / 2$$

→ $$q \sim 0.01 a^{-1}$$

which is an order of magnitude smaller than the twist needed for cohesion of rising flux tubes.

NCAR

Can α_{best} determined from photosphere vector magnetic fields be used to determined the true twist of active region flux tubes ? (Ieka et al. 2005)

- Thin flux tube assumptions:

$$\alpha_{best} = 2q$$

$$T = ql = \frac{\pi d}{2}\frac{\alpha_{best}}{2}$$

- However, flux tubes at photosphere are not thin.

  consider e.g. the simple Gold Hoyle flux tube:

$$B_z = B_0/(1+q^2r^2)$$

$$B_\theta = qrB_z$$

$$\alpha(r) = 2q/(1+q^2r^2)$$

- α_{best} corresponds to an average of α and tends to under-estimate $2q$

NCAR

Post Emergence Evolution of Active Region Flux Tubes

- Establishment of hydrostatic equilibrium along the field lines of the emerged flux tube will cause the flux tube to lose pressure confinement (i.e. B → 0) at some depth below the surface depending on the field strength at the base of the convection zone (e.g. Fan, Fisher & McClymont 1994; Moreno-Insertis et al. 1995)

$$\frac{dp_i}{dz} = -\rho_i g$$

$$\frac{dp_e}{dz} = -\rho_e g$$

$$p_e - p_i = \frac{B^2}{8\pi}$$

$$\Longrightarrow$$

$$\frac{d}{dz}\left(\frac{1}{\beta}\right) = \frac{1}{H_p}\frac{\delta T}{T_e}$$

where $\beta \equiv p_e/(B^2/8\pi)$, $\delta T \equiv T_e - T_i$.

Adiabatic flux tube:

$$\delta T(z) = \delta T(0) - \int_0^z \frac{\mu g}{R}(\nabla - \nabla_{\rm ad})dz$$

$$\rho_i(0) = \rho_e(0) \Longrightarrow \delta T(0) = \frac{1}{\beta(0)}T_e(0)$$

Therefore given $1/\beta(0)$ at the base of the convection zone, the height variation of $1/\beta(z)$ is determined.

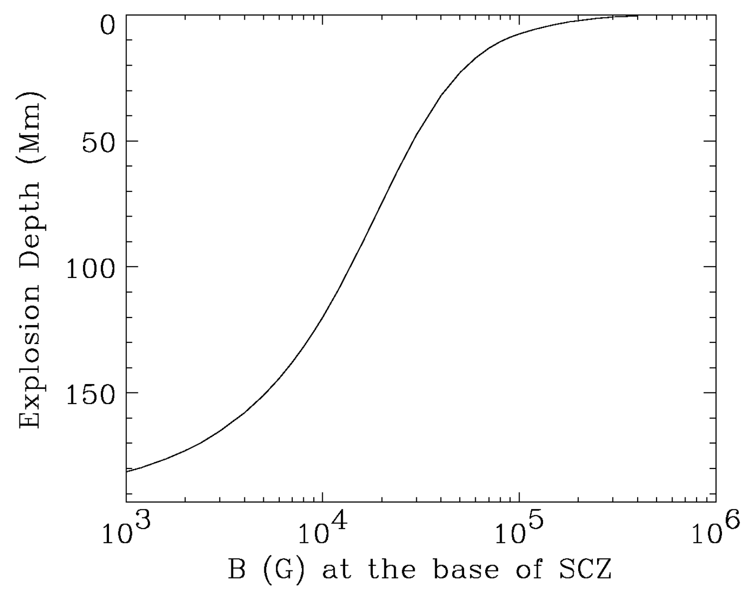

NCAR

Post Emergence Evolution of Active Region Flux Tubes

The dynamic disconnection of sunspots from their magnetic roots

(Schuessler and Rempel 2005, A&A, in press)

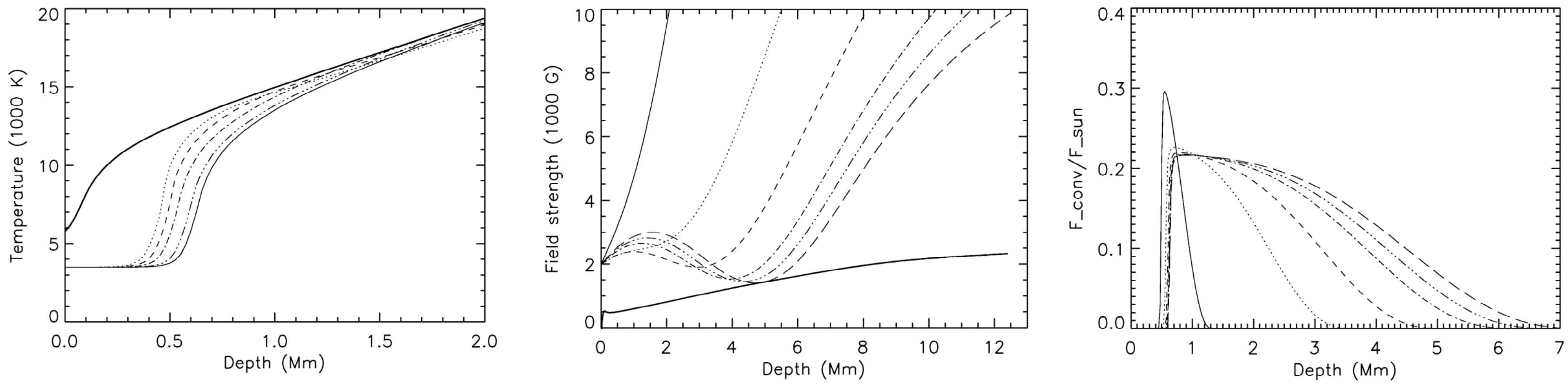

– Consider a sequence of hydrostatic, self-similar flux tube solutions that evolve quasi-statically under the influence of near surface radiative cooling, convective energy transport, and the pressure buildup due to an inflow of high entropy plasma from the lower boundary of the model flux tube.

– The combination of pressure build up by the upwelling of high entropy plasma combined with the cooling of the top layers due to radiative losses at the surface lead to a progressive weakening of the flux tube field strength at a depth of several mega-meters, and thus result in a ``dynamic disconnection'' of the emerged surface sunspots from its interior roots.

– Disconnection takes place in a depth between 2 to 6 Mm and in a time scale of less than 3 days.

NCAR

Summary and Conclusions

Preliminary 3D anelastic MHD simulations of the buoyant rise of Ω-shaped flux tubes in a rotating spherical model solar convective envelope show:

- Tubes with 50 – 100 kG field rise nearly radially to the surface, developing tilt angles consistent with Joy's law
- A field strength asymmetry develops with a stronger field strength for the leading side of the emerging tube, due to the asymmetric stretching of the flux tube by the Coriolis force induced motion. The asymmetry is more significant for flux tubes with weaker initial field strength. For 50 kG flux tube the following tube cross-section is significantly more spread out and deformed compared to the compact leading cross-section.
- Untwisted flux tube becomes too severely fragmented to be inconsistent with the emergence of solar active regions.

Quantitative calculations of a sequence of self-similar magneto-static flux tube solutions show that after the flux tube has emerged to the photosphere, the radiative cooling near the surface, combined with the upflow of high entropy plasma from below as the tube plasma establishing hydrostatic equilibrium along the field line cause a catastrophic weakening of the field strength at about 2-6 Mm depth in a time period less than 3 days, leading to a dynamic disconnection of the sunspot from its interior magnetic root.

Future work

- Self-consistently model the formation and rise of buoyant flux tubes from the base of the solar convection zone, incorporating results from the mean-field dynamo models as input:
  - What are the instabilities that can lead to the formation of active region scale flux tubes, e.g. magnetic buoyancy instabilities (modified by solar rotation)?
  - What determines the twist of the magnetic flux tubes that form, given the current helicity of the magnetic fields generated by the dynamo?
  - Properties of the emerging tube.
- Incorporating convection into the simulations.